IEEE Access
Multidisciplinary | Rapid Review | Open Access Journal

Received 21 January 2023, accepted 6 February 2023, date of publication 13 February 2023, date of current version 22 February 2023.

Digital Object Identifier 10.1109/ACCESS.2023.3244578

RESEARCH ARTICLE

A Direct Near-Field Observation of Conversion Between Waveguide Modes and Leaky Modes in Periodic Metal Structures

CHIA HO WU[1], ZHENYU QIAN[1], WEI WANG[1], JIANQI SHEN[2], XIANQING LIN[1], LI-YI ZHENG[3], FANG HE[4], (Senior Member, IEEE), XIAOLONG WANG[1,5], ZHUOYUAN WANG[6], SONG TSUEN PENG[7], (Life Fellow, IEEE), GUOBING ZHOU[4], LINFANG SHEN[1], YUN YOU[1], AND HANG ZHANG[1]

[1]Department of Applied Physics, College of Science, Zhejiang University of Technology, Hangzhou 310023, China
[2]Centre for Optical and Electromagnetic Research, College of Optical Science and Engineering, Zijingang Campus, Zhejiang University, Hangzhou 310058, China
[3]Department of Electrical Engineering, Chung Hua University, Hsinchu 30012, Taiwan
[4]Zhejiang Zhaolong Interconnect Technology Company Ltd., Deqing, Huzhou 313200, China
[5]Key Laboratory of Quantum Precision Measurement of Zhejiang Province, College of Science, Zhejiang University of Technology, Hangzhou 310023, China
[6]Electronic and Information Engineering College, Ningbo University of Technology, Ningbo 315000, China
[7]Department of Electrical Engineering, National Yang Ming Chiao Tung University, Hsinchu 30012, Taiwan

Corresponding authors: Hang Zhang (Physzhang@zjut.edu.cn) and Jianqi Shen (jqshen@zju.edu.cn)

This work was supported in part by the National Natural Science Foundation of China under Grant 62075197, Grant 62101496, Grant 61875175, Grant 62105282, and Grant 11974312; in part by the Natural Science Foundation of Zhejiang Province (Zhaolong Interconnect Technology) under Grant LQ21F010013, Grant LZ22F040005, and Grant KYY-20220693; and in part by the Ministry of Science and Technology in Taiwan under Grant MOST 103-2221-E-216-001.

ABSTRACT In order to directly observe the conversion between guided-wave modes and leaky-wave modes in a periodic structure, quadrilateral periodic metal diaphragms arranged in two ways on metal surfaces were analyzed. In the first scheme, each unit cell in the periodic structure contains a metal diaphragm, of which the dispersion characteristics of periodic structures were analyzed by the finite element method. The results of the numerical simulation show that by adjusting lattice constants of periodic structures and geometrical parameters of metal diaphragms, the transmission bandwidth of the present 1-D periodic metal diaphragm structures could be limited to X-band, where the transmission characteristics are easy to be measured. In the second scheme, a pair of mirror-symmetric and staggered quadrilateral metal diaphragms is introduced into a unit cell. It can be found in the theoretical calculation that a new dispersion curve, which passes through the light line in a high frequency range, can be exhibited. The propagation constants of dispersion curves become complex numbers and provide highly directional electromagnetic radiation that scans as the frequency changes. After the relative positions of the two metal diaphragms were properly adjusted, the frequency range of the forbidden band gap between two dispersion curves can be minimized, so as to increase the transmission bandwidth of the 1-D periodic metal structures. The experimentally measured results show that the dispersion curves of the two periodic structures were highly consistent with the theoretical results. The narrowing of the band gap could be verified by measuring the *S*-parameters. The near-field measurement of the periodic metal structures can demonstrate the conversion between the guided-wave modes and the leaky-wave modes, and the far-field measurement can show the frequency dependence of beam elevation. We expect that these artificial material structures could be widely used for designing new microwave and terahertz band devices.

INDEX TERMS Periodic metal structures, leaky mode, transmission lines.

The associate editor coordinating the review of this manuscript and approving it for publication was Ladislau Matekovits.

I. INTRODUCTION

The interaction between various periodic structures and electromagnetic waves in different frequency ranges has long

received intensive attention from many researchers, and periodic structures have been used in a number of different applications in microwave and optics. In the early stage, periodic metal diaphragms were introduced into waveguide tubes to form slow wave structures, and periodic structures could be used to reduce EM wave velocity and to couple energy to electron beams. Based on this theory, some slow wave structures and filters have been studied in detail [1], [2]. On the other hand, studies on guided-wave structures for periodically modulating reactance surfaces have been gradually carried out and some studies have been performed on the leaky-wave radiation provided by periodically loaded slow wave structures [3].

In the research field of optics, due to the progress of coating and etching technology, periodic structures can be miniaturized and employed in optical systems. Therefore, the phenomena of light waves in periodic structures, such as transmission and scattering, have been widely studied. Preliminary subjects have been considered on the issue that the mechanism of electromagnetic scattering of gratings can be used to diffract electromagnetic waves at different frequencies [4]. In integrated optics, dielectric grating couplers have replaced lenses and prisms for coupling beams to optical waveguides [5]. In the optical circuit, effective refractive indexes have been periodically designed in optical films, and the narrow-band filtering that can provide signals in integrated optical circuits at a suitable periodic interval has been selected [6]. Since sound waves propagate through mediums, mediums will produce elastic deformation that periodically changes over time and space corresponding to sound waves, which periodically disturbs refractive indexes of mediums. The disturbed mediums are equivalent to phase gratings that can diffract beams [7]. In semiconductor lasers with heterostructures, the distributed feedback (DFB) structures have attracted much attention for their significant advantages [8]. There are periodic structures outside active regions of DFB lasers, and the mirrors at both ends of lasers are replaced by periodic waveguides to realize total reflection. Photolithography is adopted to produce chrome-gold interdigital circuits on waveguide surfaces, and the voltage applied between the interleaved fingers generates periodic electric fields. Periodic changes in refractive indexes caused by electric fields will produce Bragg gratings that make beams diffract [9]. Multiplexers may drastically increase the information capacities of optical waveguides. Gratings whose periods vary with positions are used on surfaces of dielectric waveguides to deflect different wavelength beams at different waveguide positions and form demultiplexers [10].

Periodic structures play an important role in printed circuit boards (PCB). PCB design engineers reduce areas of circuit boards with various periodically distributed serpentine delay lines [11], [12]. In addition, periodic serpentine lines or periodic microstrip lines can be introduced between two parallel microstrip lines to block electromagnetic interference between two signal traces [13], [14], [15]. Recent studies have found that periodic structures etched on metal surfaces lead to new guided-wave modes [16], [17].

Due to the periodic arrangement of metal or dielectric mediums in space, the transmission of electromagnetic waves in periodic structures is similar to the forbidden band formed by electrons in periodically arranged atoms in semiconductors. Metal or materials with different refractive indexes are periodically distributed in space to form materials with band gaps similar to semiconductors [18], [19], [20], [21], [22]. Many recent artificial materials are composed of a number of continuously distributed periodic units. After these periodic units are arranged in a smart way, artificial materials with complete band gaps [23] or maximum band gaps [24] and photonic integrated circuits with all-photonic crystal structures can be obtained [25]. Some interesting physical phenomena, such as omnidirectional negative refraction [26], [27], super-prism effect [28], and birefringence [29], have been revealed in artificial materials. These artificial materials may become candidates for designing new devices due to their properties that conventional materials do not have.

Recently, the leakage behavior of many new periodic structures has received much attention of researchers. In the literature [30], [31], [32], the technique of fast-wave leaky waves of broadside radiation ability with robustness has been developed. Most of these studies were explored based on leaky wave antennas of spoof surface plasmon polaritons, where by steering the transmitted signal frequency, the field intensity of the leakage wave beam depending on the frequency can be scanned. Less attention has been paid on the interaction between electromagnetic waves and staggered mirror-symmetric 1- D periodic metal diaphragm structures. Such periodic metal structures are the focus of this work, for they have richer physical properties than periodic structures with one metal diaphragm in a unit cell. In the first part of this research, the dispersion relation of propagation mode of 1-D unilateral quadrilateral metal diaphragm arrays on metal surfaces was studied. In order to increase the transmission frequency bandwidth of electromagnetic waves propagating along 1- D unilateral array quadrilateral periodic metal diaphragms, staggered mirror-symmetric quadrilateral metal diaphragms could be introduced in the middle of two continuous quadrilateral metal diaphragms. The basic modes of the two 1-D periodic metal diaphragm array structures were studied, and the interactions between the electromagnetic fields and the two periodic structures were explored theoretically, especially the propagation characteristics and field distribution of the modes. In the second part of this study, metal aluminum was used to construct artificial materials composed of 1-D staggered metal diaphragm arrays. Compared with artificial materials composed of periodically arranged unilateral quadrilateral metal diaphragms, new dispersion curves were introduced into the waveguide structures of periodically staggered quadrilateral metal plates. By adjusting the relative positions of mirror-symmetric metal diaphragms, the band

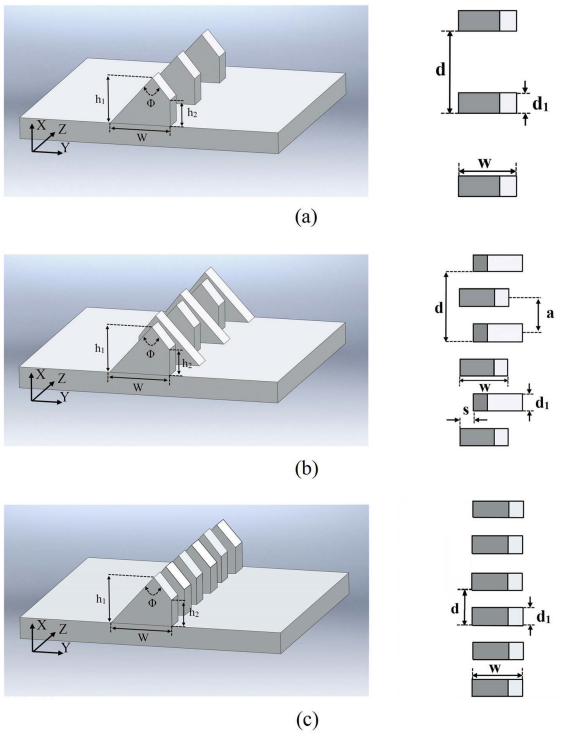

FIGURE 1. Diagram of unit cells of 1-D quadrilateral periodic metal diaphragm array structures: (a) a 1-D non-orthogonal unilateral quadrilateral periodic metal diaphragm array structure (UQPM) with the lattice constant *d*, (b) a 1-D staggered non-orthogonal quadrilateral periodic metal structure (SQPM) with the lattice constant *d*, and (c) a 1-D non-orthogonal unilateral quadrilateral periodic metal diaphragm array structure (UQPM) with the lattice constant *d* (The lattice constant of this periodic metal structure is half that of the structure in Fig. 1(a)).

gap width of periodic metal structures could be effectively reduced and the transmission bandwidth of electromagnetic waves could be increased. Dispersion curves in new propagation modes would enter radiation zones after passing through light lines and provide highly directional beams that scan when the frequency changes. By measuring the *S*-parameters, the transmission bandwidth of guided-wave modes of two kinds of metal periodic structures will be analyzed. Directional beam scanning angles were obtained by measuring the far-field radiation of leaky-wave modes. The conversion between guided-wave modes and leaky-wave modes could be directly observed from the near-field measurement.

II. THEORETICAL ANALYSIS

Two types of 1-D quadrilateral periodic metal diaphragm array structures that will be considered in this study are shown in Fig. 1. In Fig. 1(a), non-orthogonal unilateral quadrilateral metal sheets were arranged on a metal plate in a 1-D array. This periodic metal structure could restrain the electromagnetic field effectively and transmit electromagnetic signals without any dielectric materials. Due to the periodic structure, its dispersion characteristics could be expected to have electromagnetic band gaps. According to the concept proposed by Pendry et al. [16], such 1-D periodic metal array structures can efficiently constrain electromagnetic waves in a certain frequency range based on the size and shape of selected unit cells. The lattice constant of the periodic metal structure in Fig. 1(a) is represented as d, and the geometric parameters of the quadrilateral metal diaphragm are respectively represented by the following symbols: the bottom width of the metal diaphragm in the unit cell is w, the height from the bottom to the top is h_1, the thickness of the metal diaphragm is d_1, and the apex angle is Φ. The top view of the structure is on the right side of Fig. 1(a). Fig. 1(a) can be regarded as a special artificial material. Numerical methods and experimental measurements were adopted in this study in order to analyze the transmission effect of artificial materials on the electromagnetic field and obtain the transmission frequency bandwidth. Because the entire structure is made of metal materials (actually it can be realized by aluminum), it can be realized only by CNC machining. On the other hand, it can be scaled down and may become a transmission line in a monolithic integrated circuit in subterahertz or terahertz frequency band by plasma etching. Another artificial material structure is shown in Fig. 1(b). In this periodic metal structure, two metal diaphragms are mirror-symmetric along the y direction and staggered in the z direction in each unit cell. The two metal diaphragms were staggered with each other by a short distance s, with a spacing of a - d_1. The top view of the periodic metal structure is on the right side of Fig. 1(b). Such a periodic metal structure can change the width of the electromagnetic band gap by adjusting the arrangement of quadrilateral metal diaphragms. In order to thoroughly understand the interaction between these periodic metal structures and the electromagnetic fields, the finite element method was used to calculate the dispersion curves and electromagnetic field distribution of these periodic structures. The positions of the quadrilateral metal diaphragms in each unit cell in Fig. 1(b) can be continuously adjusted to change the dispersion characteristics; but under optimal conditions, only the simplest cases were selected for analysis in this work.

In Fig. 2(a) it shows the dispersion curves of a 1-D unilateral quadrilateral periodic metal diaphragm array structure in Fig. 1(a). The dispersion characteristics of the periodic metal structure were solved by COMSOL (FEM) under the periodic boundary conditions. The dispersion curves of the periodic structure were plotted in the first Brillouin zone. For numerical analysis, geometric parameters of $d = 10$ mm, $w = 7$ mm, $h_1 = 5.5$ mm, $h_2 = 3$ mm, $d_1 = 2.5$ mm, and $\Phi = 80.93°$ were selected for the periodic metal diaphragm structure in Fig. 1(a). The results of numerical analysis show that this study only treated one propagation mode in the considered frequency range. The calculated model assumed that the periodic metal structure was made of perfect conductor materials without ohmic losses. Since the calculated frequency range was in the microwave frequency band (especially in the X-band range), it was acceptable to use a model of perfect conductor for approximately describing the metal in the microwave and terahertz bands. In the model, the cutoff frequency is $f_{UQPC1} = 9.52794$ GHz

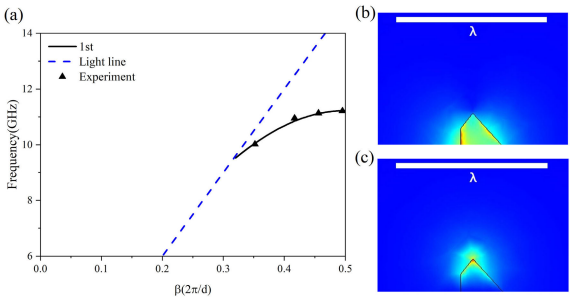

FIGURE 2. The dispersion curves and field distribution: (a) the dispersion curve of a 1-D unilateral quadrilateral metal diaphragm array with lattice constant $d = 10.0$ mm, heights $h_1 = 5.5$mm, $h_2 = 3.0$mm, metal diaphragm thickness $d_1 = 2.5$ mm and apex angle $\Phi = 80.93°$ (b) the magnetic field distribution; at the asymptotic frequency; (c) the electric field distribution at the asymptotic frequency.

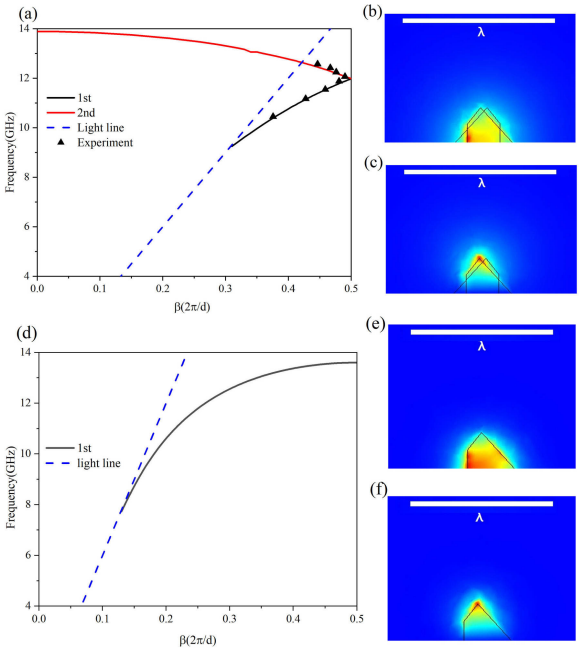

FIGURE 3. The dispersion curves and field distribution: (a) the dispersion curve of the 1-D staggered quadrilateral metal diaphragm array of lattice constant $d = 10.0$ mm; (b) the magnetic field distribution at the asymptotic frequency; (c) the electric field distribution at the asymptotic frequency; (d) the dispersion curve of a 1-D unilateral quadrilateral metal diaphragm array with lattice constant $d = 5.0$ mm; (e) the magnetic field distribution at the asymptotic frequency; (f) the electric field distribution at the asymptotic frequency.

and the asymptotic frequency is $f_{UQPA1} = 11.22291$ GHz ($\beta = \pi/d$). Periodic metal diaphragms were arranged on the flat metal surface, and the transmission bandwidth of the artificial material is 1.6949 GHz. In general, the transmission bandwidth and field confinement of the periodic structures can be adjusted by changing the shape of the unit cell or the lattice constant. An increase in the height h_1 of quadrangles could decrease the asymptotic frequency and exhibit the higher-order modes. A reduction in lattice constants of unit cells will increase the asymptotic frequency and transmission bandwidth or change electromagnetic field constraint abilities of metal periodic structures. The structure was optimized and this set of parameters was selected to construct a periodic metal structure, so the dispersion curves in Fig. 2(a) were not over complicated. In Fig. 2(a), the black triangle shows the experimentally measured dispersion curve. Fig. 2(b) shows the magnetic field of this waveguide mode at the asymptotic frequency. Fig. 2(c) shows the electric field distribution. Apparently, the electromagnetic field is mainly confined between two metal diaphragms in the transmission frequency range. The transmission characteristics of such a periodic metal structure can be completely determined by the dispersion curves, and the transmission bandwidth depends on the cutoff frequency and the asymptotic frequency of the dispersion curve. Here, the cutoff frequency is determined by the intersection point between the light line and the dispersion curve. No new physical phenomena can be discovered except that electromagnetic fields are constrained by the slow waves. On the other hand, this study paid attention to new phenomena of such periodic metal structures, such as negative slope dispersion, leaky-wave radiation, and the changing of electromagnetic signal transmission frequency bandwidth. In an attempt to explore new physical phenomena from the above structures, the following efforts were made. Without changing the size of quadrilateral metal diaphragms, each unit cell in the quadrilateral periodic metal diaphragm structure in Fig. 1(a) was introduced with another mirror-symmetric and staggered quadrilateral metal diaphragm. The new metal diaphragm was placed between the two metal diaphragms that were previously arranged in the same direction, namely $a = 5$ mm. Moreover, two sets of quadrilateral metal diaphragms were staggered and shifted by a distance s. The staggered periodic metal diaphragms in Fig. 1(b) were shifted by a distance s of 2 mm. At this point, the top view was on the right side of the structure. Each unit cell in the periodic waveguide structure in Fig. 1(b) had the same lattice constant d as the previous structure in Fig. 1(a). Compared with the structure in Fig. 1(a), each unit cell in the structure in Fig. 1(b) had an extra quadrilateral metal diaphragm. The mirror-symmetric metal diaphragm introduced was expected to change the transmission characteristics of the periodic metal structure, and a new dispersion curve was introduced into the previous dispersion map. Fig. 3(a) shows the dispersion curves obtained after the calculation of the periodic metal structure in Fig. 1(b) by the finite element method. The dispersion curves of the periodic structure were also plotted in the first Brillouin zone. As expected, the entire metal periodic structure had an extra dispersion curve. The new dispersion curve extended in the opposite direction to the first dispersion curve, with a negative slope, namely, negative slope dispersion. The first dispersion curve shows that the waveguide mode had a cutoff frequency of $f_{SQPC1} = 9.24556$ GHz, an asymptotic frequency of $f_{SQPA1} = 11.9789$ GHz ($\beta = \pi/d$), and a transmission frequency range of 2.7333 GHz. Compared with the dispersion curves in

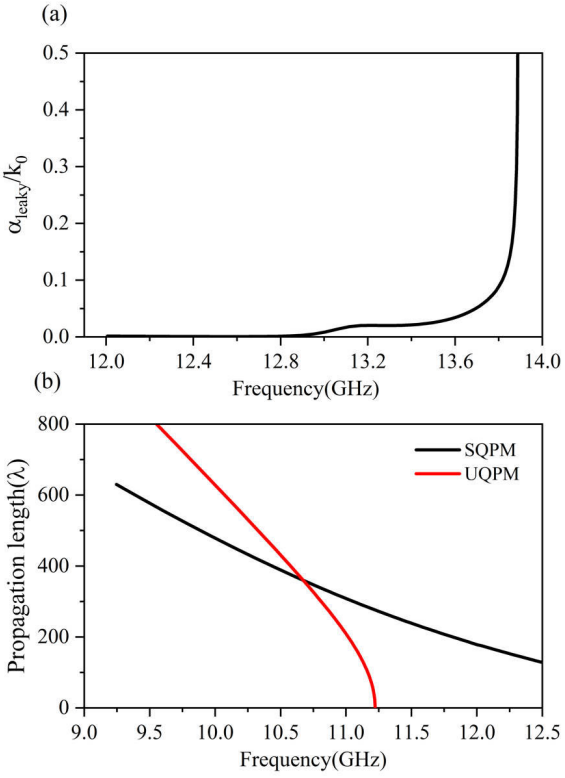

FIGURE 4. The leaky loss and propagation lengths of the periodic metal diaphragm structure: (a) the normalized imaginary part α_{leaky} /k_0 of the staggered quadrilateral periodic metal diaphragm structure in the leaky-wave frequency range; (b) the normalized propagation lengths of the unilateral quadrilateral periodic metal diaphragm structure and the staggered quadrilateral periodic metal diaphragm structure in the guided-wave frequency range.

Fig. 2(a) of the structure in Fig. 1(a), the cutoff frequency of the waveguide structure in Fig. 1(b) gradually became low, and its asymptotic frequency gradually became high, which effectively increased the transmission bandwidth of the waveguide. The dispersion curve of the first mode had a positive slope. The second dispersion curve had an asymptotic frequency of $f_{SQPA2} = 11.98346$ GHz ($\beta = \pi/d$). As the frequency of this dispersion curve increased, β decreased, indicating a negative dispersion slope. It is worth mentioning that the dispersion curves of the first and second modes had almost the same asymptotic frequency. The band gap width is only 0.036 GHz, obviously indicating that the band gap between the two modes almost disappeared. In this frequency range, this extremely small band gap had almost no effect on the propagation of electromagnetic waves. The corresponding result is that the band gap of this periodic metal structure was negligible. This phenomenon is mainly because that the reflected waves from two equally spaced sets of staggered quadrilateral metal diaphragms had a phase difference of 180° when the incident wave frequency was close to the asymptotic frequency. As a result, the two reflected waves canceled each other out, leaving only electromagnetic signals transmitting forward. The measurement results also find that at the frequency where the band gap edge is estimated to appear at $f_{SQPA2} = 11.98436$ GHz, the reflected signal is actually very small. Therefore, the first mode was directly converted to the second mode after the asymptotic frequency was exceeded. It then passed through the light line at $f = 12.64666$ GHz and entered the radiation zone to convert into a leaky-wave mode until $f = 13.89135$ GHz ($\beta = 0$). In this considered frequency range, the electromagnetic energy is gradually radiated out into space as it traveled in this mode, creating highly directional beams. As the band gap disappeared, the transmission bandwidth of the periodic metal structure increased from 2.7333 GHz to 3.4011 GHz (because the band gap was almost zero). The bandwidth of the radiation beams was 1.24469 GHz. The magnetic field distribution of unit cells is shown in Fig. 3(b) when the dispersion curve is close to the asymptotic frequency ($\beta = 0.495 \times 2\pi/d$). The electric field distribution is presented in Fig. 3(c). Apparently, each unit cell in the periodic structure had two metal diaphragms, which could restrain the electromagnetic field very efficiently. The dispersion curve calculation results of the quadrilateral metal diaphragm structure corresponding to the lattice constant $d = 5.0$ mm in Fig. 1(c) are shown in Fig. 3(d), where the cutoff and asymptotic frequencies are 7.7331 GHz and 13.602 GHz, respectively. The distribution of magnetic and electric fields of the eigen mode at the asymptotic frequency is given in Fig. 3(e) and 3(f), respectively. In order to explain how the transmission characteristics of the periodic structures can be altered by introducing the mirror-symmetric metal diaphragm with an adjacent quadrilateral diaphragm, we shall consider a quadrilateral diaphragm metal periodic structure with the lattice constant $d = 5.0$ mm, of which the dispersion curve of Fig. 1(c) is shown in Fig. 3(d). From this dispersion curve, it can be found that the cutoff frequency of the entire metal periodic structure is 7.7331 GHz and the asymptotic frequency is 13.6025 GHz. In the metal periodic structure of Fig. 1(b), the adjacent metal diaphragms exhibit a mirror-symmetry, so the lattice constant of the metal periodic structure of Fig. 1(b) is twice that of Fig. 1(c), and in Fig.1 (b), the first Brillouin zone is half that in Fig.1 (c). So the easiest way to understand the dispersion of Fig. 1(b) is that if we fold the dispersion curve of Fig. 3(d) in the range β=[0.25, 0.50]$\times 2\pi/d$ back to the first Brillouin zone, it can reduce roughly to Fig. 3(a), which is the dispersion curve corresponding to the structure of Fig. 1(b). For the metal periodic structure of Fig. 1(c), the frequency corresponding to β=0.25$\times 2\pi/d$ is f=11.79233 GHz, and the first asymptotic frequency of Fig. 1(b) is 11.9789 GHz. The asymptotic frequency of Fig. 1(c) is 13.60251 GHz, and the third asymptotic frequency of Fig. 1(b) is 13.89135 GHz. The lattice constants of the two metallic periodic structures in Fig. 1(b) and Fig. 1(c) are different, so are the slopes of the light lines, and the dispersion curve of Fig. 1(b) will pass through the light line in the high frequency range, i.e., a guided wave mode will become a leakage mode. This physical phenomenon has been clearly described as an effect of Peierls transition in solid state physics [33]. In a linear

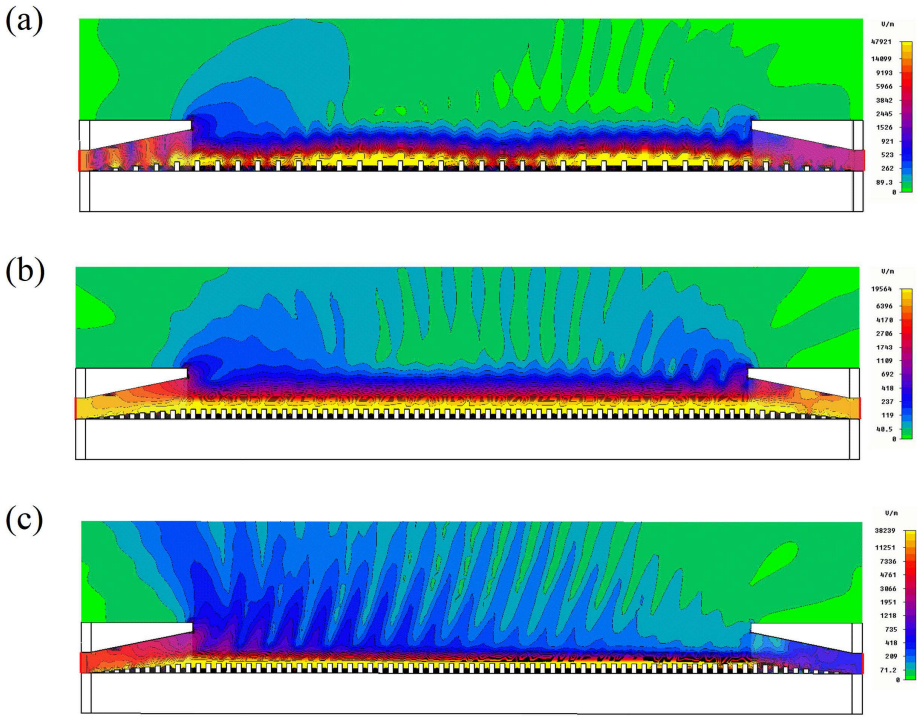

FIGURE 5. The near-field distribution of periodic metal diaphragm structures: (a) the field distribution of a unilateral quadrilateral periodic metal diaphragm structure at $\beta = 0.45 \times (2\pi/d)$ and the guided wave frequency of f = 11.09162 GHz; (b) the field distribution of a staggered quadrilateral periodic metal diaphragm structure at $\beta = 0.45 \times (2\pi/d)$ and the guided wave frequency of f = 11.44606 GHz; (c) the field distribution of a staggered quadrilateral periodic metal diaphragm structure at $\beta = 0.3 \times (2\pi/d)$ and the leaky-wave frequency of f = 13.31151 GHz.

chain of atoms, where all the atoms are equally spaced and have an interval of lattice constant d, the reciprocal space usually lies in the following interval [33].

$$-\frac{\pi}{d} < \beta < \frac{\pi}{d} \tag{1}$$

Now we change the lattice constant of the chain by moving Nr -th atom a little shift in their positions, where r is a certain integer and $N = 1, 2, 3.\ldots\ldots$, and as a result, the new lattice constant of the chain is rd. Then the order of translational symmetry of the atom chain is reduced. In this case, a unit cell will contain r atoms and the reciprocal space interval becomes the flowing form

$$-\frac{\pi}{rd} < \beta < \frac{\pi}{rd} \tag{2}$$

On the other hand, the second dispersion curve, as the frequency increased, entered the radiation zone after passing the intersection point with the light line. In the radiation zone, the propagation constant of the waveguide mode changed from a real number to a complex number with an imaginary part, i.e., $k_z = \beta + j\alpha_{leaky}$, where α_{leaky} represents the imaginary part of the propagation constant of the leaky-wave mode. This parameter α_{leaky} could be used to describe the radiation characteristics of the leakywave mode of the waveguide. The change in the normalized attenuation constant α_{leaky}/k_0 in the leaky-wave frequency range is shown in Fig. 4(a). The relation that changes with the frequency shows that α_{leaky}/k_0 was less than 5×10^{-4} before 12.67 GHz and gradually increased after 12.8 GHz (e.g.,α_{leaky}/k_0 is 16×10^{-4} at 12.838 GHz and α_{leaky}/k_0 is 0.14355 as the frequency increased to 13.852 GHz). Hence, a scanned beam was provided as the frequency changes.

Actually, all the waveguides made of real metal have certain ohmic losses. The ohmic losses affect the transmission distance of electromagnetic waves at different frequencies in periodic metal structures. It is noteworthy that the structure proposed in this study was highly innovative, with many physical properties different from those of conventional periodic structures. Therefore, for such periodic metal structures, it is very important to evaluate the imaginary part α_{loss} of the propagation constant corresponding to the conductor loss by the perturbation method [34] in the microwave frequency band. The imaginary part of this propagation constant can be expressed as $\alpha_{loss} = (P_d/P_f)/2d$, where P_f is the total power transmitted by the eigenmode in a unit cell, and P_d is the total power loss of the metal surface in a unit cell. The power loss can be calculated by integrating the metal surface. The propagation length of the mode is defined as $L = \frac{1}{2\alpha_{loss}} = (P_f/P_d)d$, and its normalized propagation length is expressed as L/λ. This physical quantity can be used to

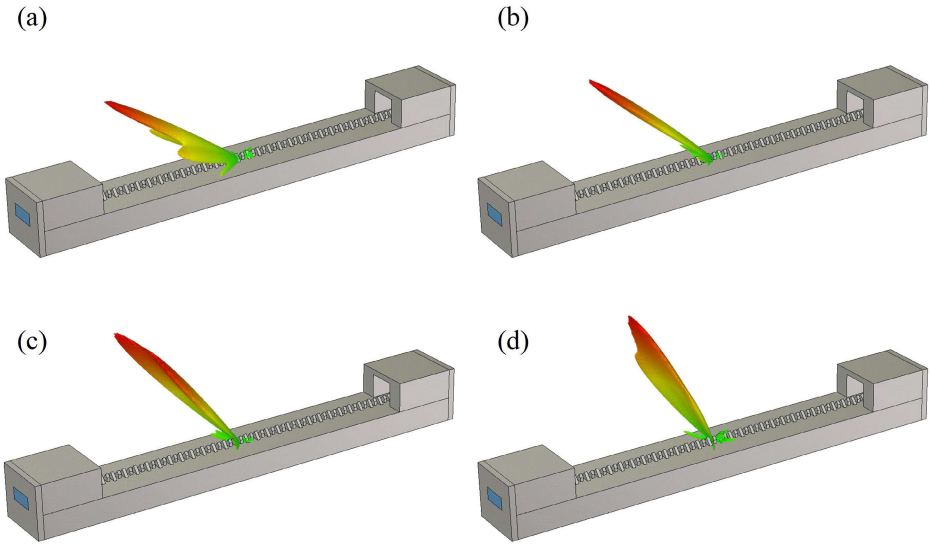

FIGURE 6. Four far-field distributions of staggered quadrilateral periodic metal diaphragm structures at a leaky-wave frequency: (a) 12.9 GHz, (b) 13.1 GHz, (c) 13.3 GHz and (d) 13.5 GHz.

calculate the effective propagation distance of electromagnetic waves at different frequencies in the periodic metal structure. The ohmic losses of the periodic metal structure composed of aluminum are considered here. The importance of propagation length lies in the limitations on the transmission of harmonic signals at different frequencies when such waveguides are used for signal transmission in practice. Fig. 4(b) shows the normalized propagation lengths of the two periodic metal structures in the guided wave frequency range. The propagation lengths of the 1-D quadrilateral periodic metal diaphragm array structure in Fig. 1(a) are calculated from the case of cutoff frequency $f_{UQPC1} = 9.52794$ GHz to the case of asymptotic frequency $f_{UQPA1} = 11.22291$ GHz in the first mode. The propagation length varies from $L/\lambda = 809.5$ at 9.52794 GHz to $L/\lambda = 0$ at the asymptotic frequency of 11.22291 GHz. For the low-frequency signals, the periodic metal structures have a low constraint on the electromagnetic field, with low ohmic losses, so the corresponding signals with long wavelength can be transmitted over a long distance in periodic metal structures. However, with the increase of the frequency, the constraint of the electromagnetic field on the metal periodic structures gradually increases, and the signals with short wavelength result in a sharp increase in ohmic losses, so that the propagation length decreases gradually until the asymptotic frequency f_{UQPA1} becomes zero. The normalized propagation length of the staggered quadrilateral periodic metal diaphragm structure in Fig. 1(b) changes from $L/\lambda = 629.9$ at the cutoff frequency of $f_{SQPC1} = 9.24556$ GHz to L/λ=183.3 at $f = 11.95627$ GHz which is close to the asymptotic frequency. The normalized propagation length of the staggered periodic metal diaphragm structure does not immediately become zero when the frequency reaches the asymptotic frequency, indicating that the band gap at $\beta = \pi/d$ is too small to affect the mode transmission. Therefore, the frequency bandwidth of electromagnetic wave propagation is $f = 12.64666$ GHz from the first to the second intersection points between the dispersion curve and the light line, when L/λ is 113.85.

The electromagnetic field distribution only in a unit cell is shown in Fig. 2 and Fig. 3. In order to investigate the transmission characteristics of periodic metal structures in detail, it is necessary to present the near-field distribution of an entire periodic metal structures in the guided-wave frequency range and the leaky-wave frequency range by the numerical method. The electric field distribution of the unilateral quadrilateral periodic metal diaphragm structure at $\beta = 0.45 \times (2\pi/d)$ and a guided wave frequency of 11.09162 GHz is shown in Fig. 5(a). The field distribution of the staggered periodic metal diaphragm structure at $\beta = 0.45 \times (2\pi/d)$ and a guided wave frequency of 11.44606 GHz is also shown in Fig. 5(b). The electric field distribution of the staggered quadrilateral periodic metal diaphragm structure in Fig. 5(b) has a higher constraint than that of the unilateral quadrilateral periodic metal diaphragm structure in Fig. 5(a). Apparently, doubled metal diaphragms have a higher constraint on the electromagnetic field. In general, the physical mechanism why such metallic diaphragm periodic structures are able to constrain the electromagnetic field more effectively with the reduction of lattice constant d can be qualitatively understood in the following manner. When the lattice constant d decreases, the number of metal diaphragms per unit length increases, so does the surface area of the metal conductor, which corresponds to the increase of the effective capacitance per unit length of the metallic periodic structure, so that the electric field lines can be trapped more effectively. On the other hand, the current flowing on

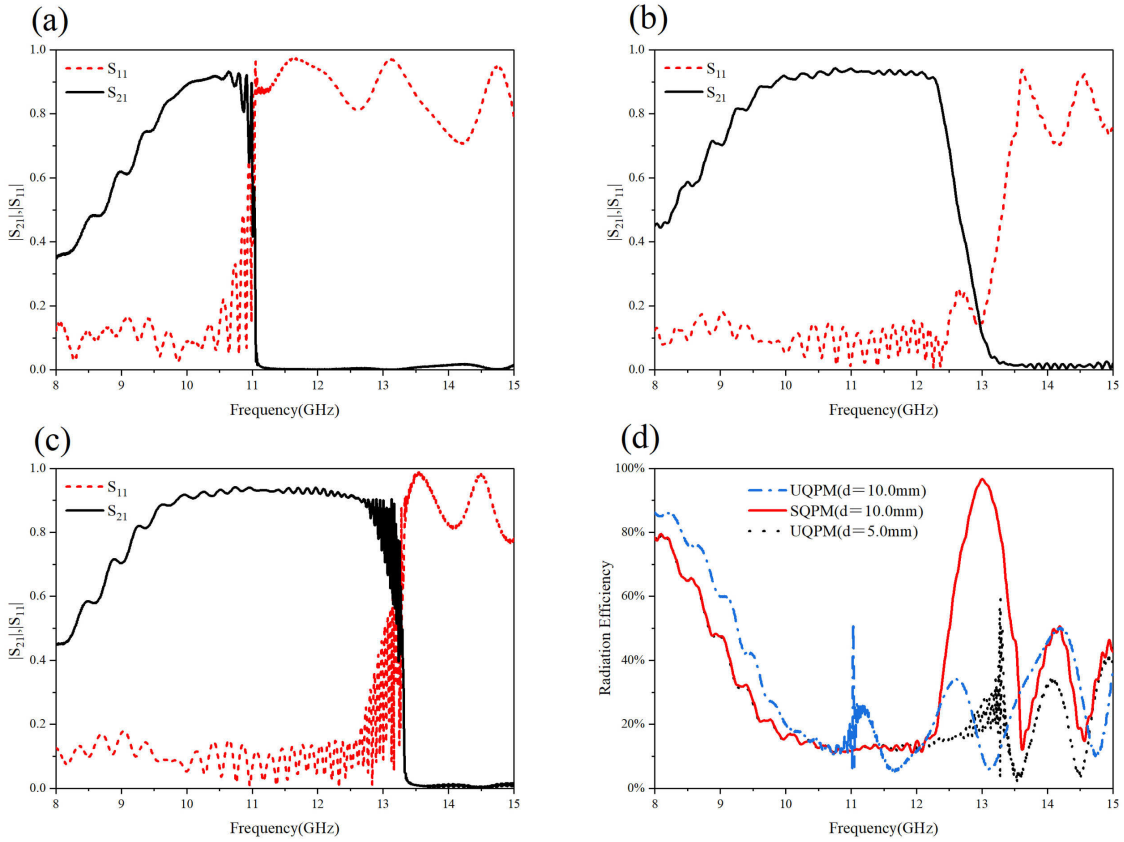

FIGURE 7. The simulation results of the *S*-parameters and radiation efficiency for the periodic metal structures: (a) the *S*-parameters of the 1-D unilateral quadrilateral metal diaphragm array with lattice constant $d = 10.0$ mm; (b) the *S*-parameters of the 1-D staggered quadrilateral metal diaphragm array of lattice constant $d = 10.0$ mm; (c) the *S*-parameters of the 1-D unilateral quadrilateral metal diaphragm array with lattice constant $d = 5.0$ mm; (d) the radiation efficiency (depending on frequency) of the three metal periodic structures.

the surface of the metal grooves is more able to attract the magnetic field lines into the grooves than in the case of long lattice constant, that is, an increase in the number of grooves corresponds to an increase in self-inductance per unit length. It can also be seen from the literature on periodic microstrip lines [18] that the reduction of lattice constant d helps to increase the self-inductance of microstrip lines. The electric field distribution of the staggered periodic metal diaphragm structure at $\beta = 0.3 \times (2\pi/d)$ and the leaky-wave frequency of $f = 13.31151$ GHz is shown in Fig. 5(c). As it is in the leaky-wave frequency band of the waveguide, a large amount of electromagnetic field radiates outside the periodic metal structure. The periodic metal structure shown in Fig. 1(b) has rarely been explored in the previous studies. Therefore, it is very important to explore the far-field distribution of this periodic metal structure in the leaky-wave frequency range.

The far-field distributions of staggered periodic metal diaphragm structures in the leaky-wave frequency range are shown in Fig. 6. The figure indicates that a very narrow main beam is generated when the electromagnetic waves are fed from the left waveguide adapter. The far-field distributions of the leaky-wave modes at 12.9 GHz and 13.1 GHz are shown in Fig. 6(a) and 6(b), respectively. According to Fig. 6, when the electromagnetic wave frequency is in the leaky-wave frequency range, the far-field distribution shows the main beam with a very narrow distribution range in space, where θ represents the elevation angle between the main beam and the horizontal direction. The elevation angle θ of the main beam increases gradually with the increasing frequency. Since the entire guided wave structure made of metal is an open type, and the corresponding scaled-down periodic metal structure may be directly used for waveguide transmission in the THz band. After we have obtained the dispersion curves of the quadrilateral metal periodic structures in Figs. 2 and 3, the radiation efficiency of the metal periodic structures can be explored according to the references [31], [36]. Based on the metal periodic structure in Fig. 1, a waveguide structure with a total length of 37.5 cm can be designed. Here, the electromagnetic numerical method is used to calculate the *S*-parameters of the waveguide structure schematically plotted in Fig. 6. Without considering the ohmic loss, the radiation efficiency can be calculated by $1\text{-}S_{11}^2\text{-}S_{21}^2$. The *S*-parameters of the three structures in Fig. 1(a)-(c) are given in Fig. 7(a)-(c), respectively, and the variation of

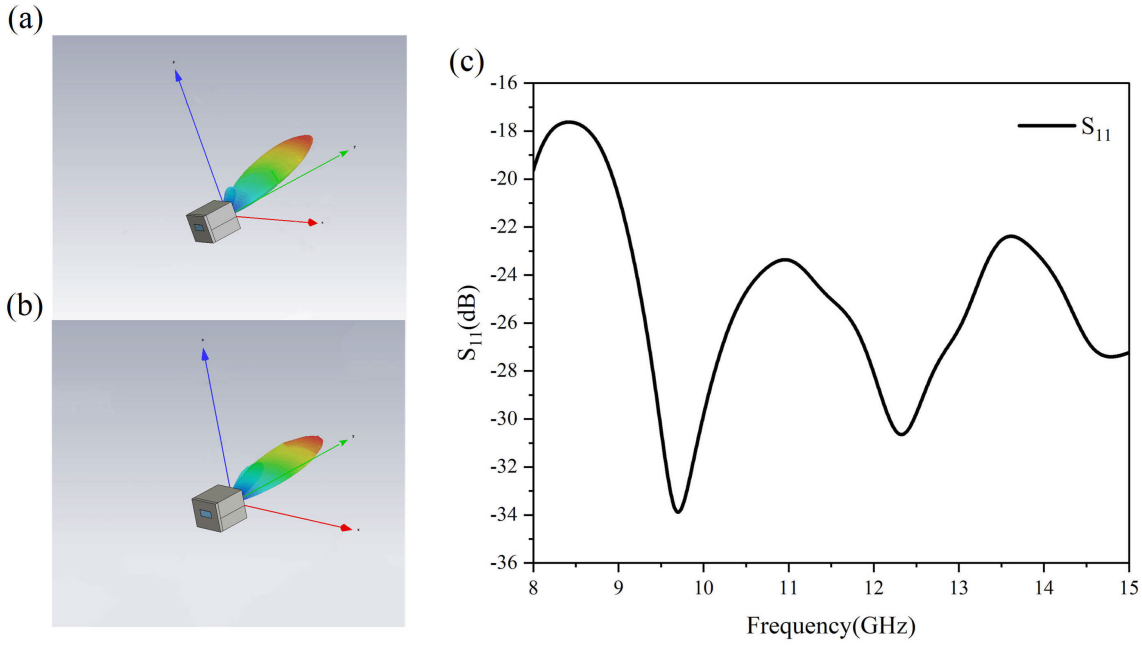

FIGURE 8. The far-field distribution and return loss of the horn-like parts of the waveguide: (a) the far-field distribution at 8 GHz; (b) the far-field distribution at 15 GHz; (c) the return loss of the horn-like part of the waveguide.

the radiation efficiency (depending on frequency) of the metal periodic structure is shown in Fig. 7(d), where it can be seen that the high efficiency of the electromagnetic radiation can be exhibited between 12.5 GHz and 13.5 GHz. Since it is necessary to analyze the strong radiation characteristics of the transition part (i.e., the horn-like parts at two terminals) of the periodic metal structure, here the numerical method is used to calculate the return loss and radiation field distribution of the horn-like parts as in reference [35], and the results are shown in Fig. 8, where the far-field radiation of the horn-like parts at 8.0 GHz and 15.0 GHz is shown in Figs.8(a) and 8(b), respectively, and the behavior of change in the return loss with frequency is given in Fig. 8(c). Then it can be seen that the transition part can provide a high radiation efficiency.

III. EXPERIMENTAL RESULTS

In order to verify the results of the above numerical simulation, the S-parameters and field distribution of the 1-D periodic metal diaphragm array structures were measured. Here, according to the structures shown in Fig. 1(a) and (b), aluminum is used to make two 1-D periodic metal di-aphragm array structures. The unit cell of the periodic metal diaphragm structure is exactly the same as the structure in Fig. 1 in shape and size, with the total length of 37.5 cm.

The network analyzer is first used to measure the S-parameters for determining the transmission characteristics of the whole waveguide. The photo of the 1-D unilateral quadrilateral periodic metal diaphragm structure is shown in Fig. 9(a). By making use of CNC machining, the entire metal diaphragm arrays on smooth metal surfaces were made of aluminum. The measured S-parameters of 1-D unilateral quadrilateral periodic metal diaphragm structure in a frequency ranging from 8 GHz to 15 GHz is given in Fig. 9(b). Here, the red dashed and solid black lines represent the curves of S_{11} and S_{21}, respectively, which change with the frequency. S_{21} characterizes the transmission of the periodic metal structures. For the unilateral quadrilateral periodic metal structure, S_{21} gradually increases from 0.31361 at 8.00 GHz to 0.8 at 10.18 GHz, with the maximum of 0.8169 at 10.58 GHz, and S_{21} can be maintained above 0.8 in the frequency range from 10.18 GHz to 10.87 GHz. Immediately after that, S_{21} decreases with the frequency and is 0.03226 at a frequency of $f = 11.27$ GHz. Before $f = 11.03$ GHz is achieved, S_{11} changes rapidly with the frequency, with the maximum less than 0.3. However, at $f = 11.22$ GHz, S_{11} increases to 0.72197, indicating that it has entered the band gap region of the unilateral quadrilateral periodic metal diaphragm structure. Apparently, the measured S-parameters is consistent with the dispersion curve calculated by the finite element method (It must be noted that due to the machining error, the measurement of S-parameters also has the frequency deviation of 0.35GHz from the theoretical simulation.). The photo of the staggered quadrilateral periodic metal diaphragm structure is presented in Fig. 9(c) and the measured S-parameters of the staggered quadrilateral periodic metal diaphragm structure is given in Fig. 9(d). The trend of S-parameters change clearly shows that S_{21} measured is 0.41461 at $f = 8.00$ GHz and 0.80239 at $f = 9.99$ GHz. At $f = 12.25$ GHz, S_{21} is measured as 0.80455. In the frequency range, the waveguide has a very high transmission

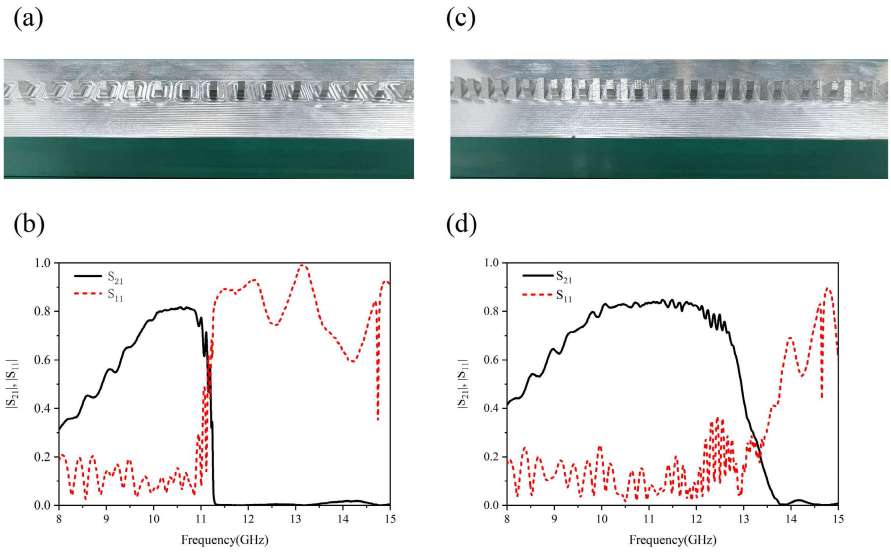

FIGURE 9. The experimental periodic metal diaphragm structures and the measured *S*-parameters: (a) the unilateral quadrilateral periodic metal diaphragm structure; (b) the measured *S*-parameters of a unilateral quadrilateral periodic metal diaphragm structure; (c) the staggered quadrilateral periodic metal diaphragm structure; (d) the measured *S*-parameters of a staggered quadrilateral periodic metal diaphragm structure.

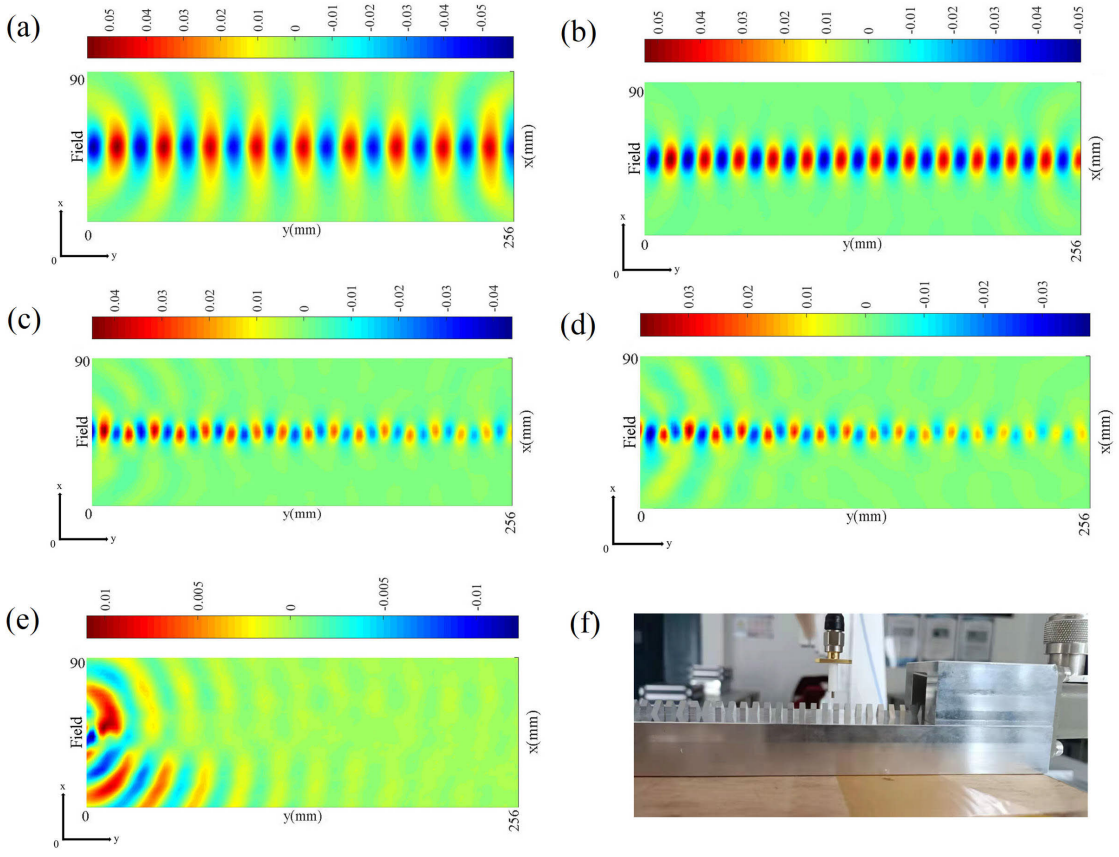

FIGURE 10. The near-field distribution of the staggered quadrilateral periodic metal diaphragm structure: the curves were measured at (a) 10.00 GHz, (b) 12.00 GHz, (c) 13.05 GHz, (d) 13.20 GHz, and (e) 14.00 GHz. The near-field experimental equipment photo is shown in panel (f).

efficiency. At $f = 11.49$ GHz, the maximum of S_{21} is 0.84797. The staggered quadrilateral periodic structure has higher transmission efficiency and bandwidth than the unilateral periodic structure. S_{11} of a staggered structure is 0.17079

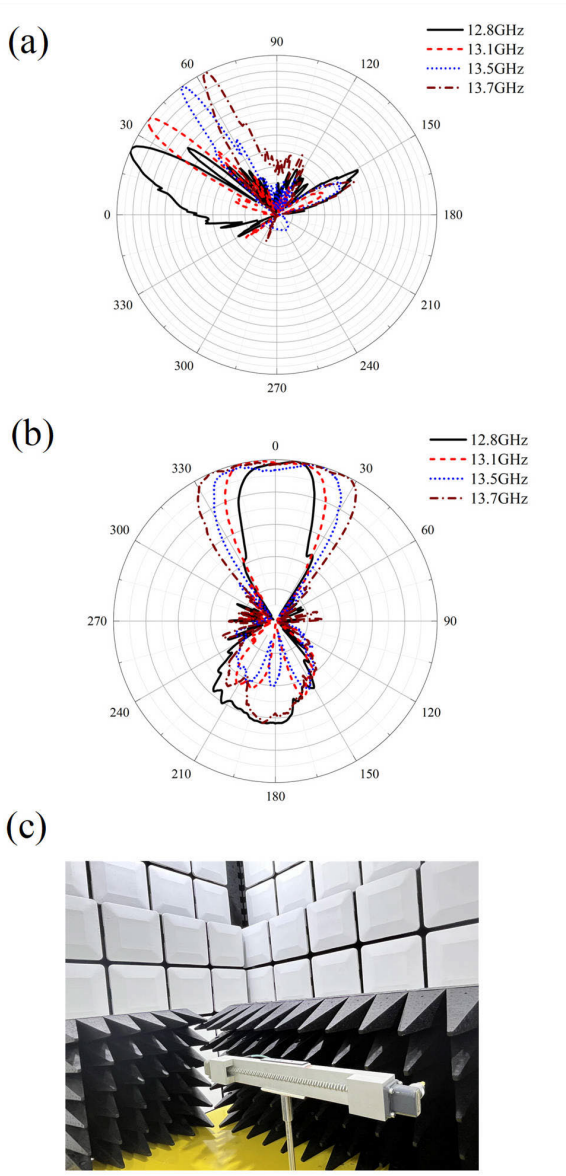

FIGURE 11. The far-field distribution of the staggered quadrilateral periodic metal diaphragm structure in the leaky-wave frequency range measured in the experiment: (a) the main beam distribution depending on the elevation angle; (b) the field pattern and azimuth distribution of the main beam; (c) the far-field experiment photo.

at $f = 8.00$ GHz, and is obviously lower than that of a unilateral structure at a frequency in the beginning. Immediately after that, S_{11} changes rapidly, increases gradually and reaches its maximum 0.39209 at $f = 12.94$ GHz. In addition, there is the biggest difference between Fig. 9(b) and Fig. 9(d): when the parameter S_{21} of the staggered periodic structure drops rapidly at 12.65 GHz, S_{11} does not rise immediately, indicating that it enters the leaky-wave frequency range of the periodic metal structure until 13.89 GHz is reached. After 13.89 GHz is reached, the parameter S_{11} gradually increases with the frequency and enters the band gap region of the staggered periodic metal structure. The entire metal periodic structure was measured in the near-field of the area with a length of 27.5 cm and a width of 9.5 cm. The near-field measurement of the staggered quadrilateral periodic metal diaphragm structure at different frequencies is shown in Fig. 10. In the guided-wave zone, the waveguide mode can maintain the complete field distribution during transmission, for example at frequency $f = 12.00$ GHz. In the leaky-wave zone, the waveguide mode gradually collapses during propagation, for example, at $f = 13.05$ GHz. It can be clearly seen here that in the frequency range of the guided-wave, the field distribution gradually shrinks inward and is confined around the metal diaphragms, forming a compact mode structure. However, it enters the frequency range of leaky wave. Afterwards, the originally compact mode structure gradually depleted energy during the propagation, and the phenomenon of field distribution, which twisted and oscillated, appeared between the metal diaphragms. Fig. 10(e) is the near-field measurement result at the frequency $f = 14.0$ GHz on the waveguide surface. Since $f = 14.0$ GHz is already located in the forbidden band of the periodic metal structure, the electromagnetic energy can no longer enter the periodic metal structure. The measurement process is shown as a photo in Fig. 10(f). The readers can refer to the Ref. [37] for the process of near-field measurement of leaky wave antenna.

In order to understand well the radiation field of the leaky wave mode, the results of far-field measurement are provided here, namely, the relationship between the main waveguide beam distribution and the elevation angle is shown in Fig. 11(a). At $f = 12.8$ GHz, the elevation angle θ of the main beam is 24° and the 3dB angle width $\Delta\theta$ of the beam is 12°; at f =13.7 GHz, the elevation angle θ of the main beam is 63° and the 3dB elevation angle width $\Delta\theta$ of the beam is 7°. Thus, from $f = 12.8$ GHz to $f = 13.7$ GHz, the beam scanning angle is 39°. On the other hand, the 3dB azimuth angle width $\Delta\phi$ of the beam increases from 29° ($f = 12.8$ GHz) to 63°($f = 13.7$ GHz) which has been shown in Fig. 11(b). As the frequency increases, the 3dB elevation angle width of the beam gradually becomes smaller and the 3dB azimuth angle width $\Delta\phi$ gradually increases. The far-field measurement process is shown as a photo in Fig. 11(c).

IV. CONCLUSION

In this work, the electromagnetic properties of a type of artificial materials with 1-D staggered quadrilateral metal diaphragm arrays have been analyzed. Generally, periodic structures will unavoidably exhibit band gap characteristics. Compared with the unit cells in periodic structures containing only a metal diaphragm, an extra dispersion curve has been found by numerical calculation. However, the band gap can be minimized by adjusting the arrangement of metal diaphragms. Such periodic metal structures can transcend the limits of band gap and improve the transmission bandwidth. After the extra dispersion curve passes the light line in a high frequency range, the propagation constant of the mode turns

out to be a complex number and provides highly directional radiation beams. The *S*-parameters of the present periodic structures measured by the network analyzer has verified that the transmission bandwidth can be increased after the band gap is minimized. The conversion between the guided-wave modes and the leaky-wave modes has been observed from the near-field measurement of the periodic structure. It is verified in the far-field measurement that the leaky-wave mode of new artificial materials can provide the beams that scan as the frequency changes.

ACKNOWLEDGMENT

The authors would like to thank Prof. Jianqing Shi and Prof. Qiang Lin for helping establishing the Microwave Measurement Laboratory, and also would like to thank Dr. Yu-Jun Zhang (H3C Technologies Company Ltd.) and Dr. Bing Cai and Hao-Hui Qiu (Hangzhou TDT Technologies Company Ltd.) for their helpful discussions in measurements.

REFERENCES

[1] J. R. Pierce, "Theory of the beam-type traveling-wave tube," *Proc. IRE*, vol. 35, no. 2, pp. 111–123, Feb. 1947.

[2] R. M. Bevensee, *Electromagnetic Slow Wave System*. New York, NY, USA: Wiley, 1964.

[3] P. Baccarelli, S. Paulotto, D. R. Jackson, and A. A. Oliner, "A new Brillouin dispersion diagram for 1-D periodic printed structures," *IEEE Trans. Microw. Theory Techn.*, vol. 55, no. 7, pp. 1484–1495, Jul. 2007.

[4] S. T. Peng, T. Tamir, and H. L. Bertoni, "Theory of periodic dielectric waveguides," *IEEE Trans. Microw. Theory Techn.*, vol. MTT-23, no. 1, pp. 123–133, Jan. 1975.

[5] S. T. Peng and T. Tamir, "Directional blazing of waves guided by asymmetrical dielectric gratings," *Opt. Commun.*, vol. 11, no. 4, pp. 405–409, Aug. 1974.

[6] R. V. Schmidt, D. C. Flanders, C. V. Shank, and R. D. Standley, "Narrow-band grating filters for thin-film optical waveguides," *Appl. Phys. Lett.*, vol. 25, no. 11, p. 651, 1974.

[7] J. M. Hammer and D. J. Channin, "Simple acoustic grating modulators," *Appl. Opt.*, vol. 10, no. 11, pp. 2203–2209, 1972.

[8] A. Yariv and M. Nakamura, "Periodic structures for integrated optics," *IEEE J. Quantum Electron.*, vol. QE-13, no. 4, pp. 233–253, Apr. 1977.

[9] J. F. S. Ledger and E. A. Ash, "Laser-beam modulation using grating diffraction effects," *Electron. Lett.*, vol. 6, no. 4, pp. 99–100, 1968.

[10] A. C. Lianos, A. Katzir, A. Yariv, and C. S. Hong, "Chirped-grating demultiplexers in dielectric waveguides," *Appl. Phys. Lett.*, vol. 30, no. 10, pp. 512–519, 1977.

[11] W.-S. Chang and C.-Y. Chang, "A high slow-wave factor microstrip structure with simple design formulas and its application to microwave circuit design," *IEEE Trans. Microw. Theory Techn.*, vol. 60, no. 11, pp. 3376–3383, Nov. 2012.

[12] G.-H. Shiue, J.-H. Shiu, Y.-C. Tsai, and C.-M. Hsu, "Analysis of common-mode noise for weakly coupled differential serpentine delay microstrip line in high-speed digital circuits," *IEEE Trans. Electromagn. Compat.*, vol. 54, no. 3, pp. 655–666, Jun. 2012.

[13] K. Lee, H.-B. Lee, H.-K. Jung, J.-Y. Sim, and H.-J. Park, "A serpentine guard trace to reduce the far-end crosstalk voltage and the crosstalk induced timing jitter of parallel microstrip lines," *IEEE Trans. Adv. Packag.*, vol. 31, no. 4, pp. 809–817, Nov. 2008.

[14] W.-T. Huang, C.-H. Lu, and D.-B. Lin, "Suppression of crosstalk using serpentine guard trace vias," *Prog. Electromagn. Res.*, vol. 109, pp. 37–61, 2010.

[15] C. H. Wu, P. Ma, G. Zhou, J. Shen, Z. Qian, L. Shen, H. Zhang, Z. Wang, X. Wang, and F. He, "An application of the subwavelength periodic microstrip guard trace in high-speed circuits," *IEEE Access*, vol. 10, pp. 42640–42655, 2022.

[16] J. B. Pendry, L. Martín-Moreno, and F. J. Garcia-Vidal, "Mimicking surface plasmons with structured surfaces," *Science*, vol. 305, no. 5685, pp. 847–848, Aug. 2004.

[17] S. A. Maier, S. R. Andrews, L. Martín-Moreno, and F. J. García-Vidal, "Terahertz surface plasmon-polariton propagation and focusing on periodically corrugated metal wires," *Phys. Rev. Lett.*, vol. 97, no. 17, Oct. 2006, Art. no. 176805.

[18] C. H. Wu, G. Zhou, P. Ma, Y. Wu, K. Li, L. Shen, Q. Shen, H. Zhang, J. Yan, Y. You, J. Shen, X. Wang, C.-C. Chang, and F. He, "Analysis of the electromagnetic interaction between periodically corrugated transmission lines through the mutual capacitance and mutual inductance," *IEEE Access*, vol. 10, pp. 15818–15834, 2022.

[19] C. H. Wu, G. Zhou, J.-Y. Juang, Q. Shen, Y. You, J. Yan, L. Shen, H. Zhang, Y. Wu, F. Zhu, and C. C. Chang, "Circuit model of parallel corrugated transmission lines for differential signal propagating in microwave band," *IEEE Access*, vol. 8, pp. 221783–221793, 2020.

[20] E. Yablonovitch, "Inhibited spontaneous emission in solid-state physics and electronics," *Phys. Rev. Lett.*, vol. 58, no. 20, pp. 2059–2062, May 1987.

[21] S. John, "Strong localization of photons in certain disordered dielectric superlattices," *Phys. Rev. Lett.*, vol. 58, pp. 2486–2489, Jun. 1987.

[22] J. D. Joannopoulos, S. G. Johnson, J. N. Winn, and R. D. Meade, *Photonic Crystals: Molding the Flow of Light*, 2nd ed. Princeton, NJ, USA: Princeton Univ. Press, 2008.

[23] K. M. Ho, C. T. Chan, and C. M. Soukoulis, "Existence of a photonic gap in periodic dielectric structures," *Phys. Rev. Lett.*, vol. 65, no. 25, pp. 3152–3155, Dec. 1990.

[24] S. Fan, P. R. Villeneuve, and J. D. Joannopoulos, "Large omnidirectional band gaps in metallodielectric photonic crystals," *Phys. Rev. B, Condens. Matter*, vol. 54, no. 16, pp. 11245–11251, Oct. 1996.

[25] S.-Y. Lin, E. Chow, V. Hietala, P. R. Villeneuve, and J. D. Joannopoulos, "Experimental demonstration of guiding and bending of electromagnetic waves in a photonic crystal," *Science*, vol. 282, no. 5387, pp. 274–276, Oct. 1998.

[26] M. Notomi, "Theory of light propagation in strongly modulated photonic crystals: Refractionlike behavior in the vicinity of the photonic band gap," *Phys. Rev. B, Condens. Matter*, vol. 62, no. 16, pp. 10696–10705, Oct. 2000.

[27] C. Luo, S. G. Johnson, J. D. Joannopoulos, and J. B. Pendry, "All-angle negative refraction without negative effective index," *Phys. Rev. B, Condens. Matter*, vol. 65, no. 20, May 2002, Art. no. 201104.

[28] H. Kosaka, T. Kawashima, A. Tomita, M. Notomi, T. Tamamura, T. Sato, and S. Kawakami, "Superprism phenomena in photonic crystals," *Phys. Rev. B, Condens. Matter*, vol. 58, no. 16, pp. R10096–R10099, Oct. 1998.

[29] K. Sakoda, *Optical Properties of Photonic Crystal*. Berlin, Germany: Springer-Verlag, 2001, pp. R1096–R1099.

[30] G. S. Kong, H. F. Ma, B. G. Cai, and T. J. Cui, "Continuous leaky-wave scanning using periodically modulated spoof plasmonic waveguide," *Sci. Rep.*, vol. 6, no. 1, p. 29600, Jul. 2016.

[31] Z. Xu, X. Zhang, S. Li, H. Zhao, and X. Yin, "Leaky-wave radiation from periodically modulated spoof surface plasmon polaritons," in *Proc. 6th Asia–Pacific Conf. Antennas Propag. (APCAP)*, Oct. 2017, pp. 1–3.

[32] L. Liu, M. Chen, J. Cai, X. Yin, and L. Zhu, "Single-beam leaky-wave antenna with lateral continuous scanning functionality based on spoof surface plasmon transmission line," *IEEE Access*, vol. 7, pp. 25225–25231, 2019.

[33] R. E. Peierls, *Quantum Theory of Solids*. London, U.K.: Oxford Univ. Press, 1955, pp. 108–112.

[34] L. Shen, X. Chen, Y. Zhong, and K. Agarwal, "Effect of absorption on terahertz surface plasmon polaritons propagating along periodically corrugated metal wires," *Phys. Rev. B, Condens. Matter*, vol. 77, no. 7, Feb. 2008, Art. no. 075408.

[35] Z. Xu, M. Wang, S. Fang, H. Liu, Z. Wang, and D. F. Sievenpiper, "Broadside radiation from Chern photonic topological insulators," *IEEE Trans. Antennas Propag.*, vol. 70, no. 3, pp. 2358–2363, Mar. 2022.

[36] Z. Xu, S. Li, X. Yin, H. Zhao, and L. Liu, "Radiation loss of planar surface plasmon polaritons transmission lines at microwave frequencies," *Sci. Rep.*, vol. 7, no. 1, p. 6098, Jul. 2017.

[37] Z. Xu, J. Tong, T. J. Cui, J. Chang, and D. F. Sievenpiper, "Near-field chiral excitation of universal spin-momentum locking transport of edge waves in microwave metamaterials," *Adv. Photon.*, vol. 4, no. 4, Jul. 2022, Art. no. 046004.

CHIA HO WU was born in Tainan, Taiwan. He received the M.S. degree in physics from the National Tsing Hua University, Hsinchu, Taiwan, in 1987, and the Ph.D. degree in electro-optics from the National Chiao Tung University, Hsinchu, in 1997. He has been a Professor with the Department of Applied Physics, College of Science, Zhejiang University of Technology, Hangzhou, China, since 2018. His research interests include propagation and scattering of dielectric waveguides, numerical analysis of dielectric gratings, active leaky wave antennas, and subwavelength periodic metal structures.

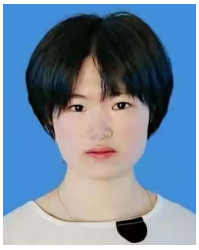

ZHENYU QIAN was born in Ningbo, Zhejiang, China, in 2000. She received the B.S. degree from the Zhejiang University of Technology, Zhejiang, in 2022, where she is currently pursuing the master's degree. Her research interests include metamaterials, crosstalk analysis of high-speed signal, and antenna design.

WEI WANG was born in Tianshui, Gansu, China, in 1998. He received the B.S. degree from the Zhejiang University of Technology, Zhejiang, China, in 2022, where he is currently pursuing the master's degree. His research interests include microstrip antenna design, millimeter-wave, micro-nano devices, and subwavelength periodic metal structures.

JIANQI SHEN was born in Xiaoshan, Hangzhou, Zhejiang, China, in November1974. He received the Ph.D. degree from the Joint Research Centre of Photonics, Royal Institute of Technology, Sweden, and Zhejiang University, China. He was a Postdoctoral Researcher at Zhejiang University, from 2006 to 2008. He is currently an Associate Professor with the College of Optical Science and Engineering, Zhejiang University. His research interests include surface plasmonics, electromagnetic metamaterials, quantum optics, and related theoretical topics in classical and quantum field theories.

XIANQING LIN received the B.S. degree in applied physics from the China University of Petroleum, Dongying, China, in 2009, and the Ph.D. degree in physics from Tsinghua University, Beijing, China, in 2014. His research interest includes electronic and optical properties of low dimensional materials.

LI-YI ZHENG was born in Hsinchu, Taiwan, in 1991. He received the B.S. and M.S. degrees from Chung Hua University, Hsinchu, in 2014 and 2016, respectively. His research interests include leaky wave antennas, subwavelength periodic metal structures, and design of semiconductor instruments.

FANG HE (Senior Member, IEEE) received the B.Eng. degree in communication engineering from Jilin University, Changchun, China, in 2002, and the M.Sc. degree in communication engineering and the Ph.D. degree in electrical and electronics engineering from The University of Manchester, Manchester, U.K., in 2005 and 2011, respectively. He had been with HellermannTyton Data Ltd., Northampton, U.K., since 2009, where he was the Product Development Engineer. Since 2019, he has been with Zhejiang Zhaolong Interconnect Technology Company Ltd., Deqing, China, where he is currently the Chief Specialist of generic cabling and the Laboratory Director. He is a member of the Institution of Engineering and Technology (IET), U.K. He is also a Chartered Engineer from the Engineering Council, U.K.

XIAOLONG WANG was born in Qingdao, China. He received the B.S. degree in physics and the Ph.D. degree in optics from Zhejiang University, in 2006, and the Ph.D. degree in physics from Paris Observatory, in 2011. For his Ph.D. degree, he followed the agreements between the Ministry of Education of China and the Ministry of Education of France. Since 2014, he has been working as an Assistant Professor with the College of Science, Zhejiang University of Technology. His research interests include atom interferometry, optical spectroscopy, and metamaterials.

ZHUOYUAN WANG is currently a Professor with the Electronic and Information Engineering College, Ningbo University of Technology. He majored in electronic science and technology at Zhejiang University. He has undertaken two projects of the Natural Science Foundation of Zhejiang Province and several projects of the Natural Science Foundation of Ningbo. He has published more than 20 professional papers. His research interests include electromagnetic field theory, metamaterials, electromagnetic structure design, and RF device design and optimization.

SONG TSUEN PENG (Life Fellow, IEEE) was born in Taiwan, in February 1937. He received the B.S. degree in electrical engineering from the National Cheng Kung University, Hsinchu, Taiwan, in 1959, the M.S. degree in electronics from the National Chiao Tung University, Hsinchu, in 1961, and the Ph.D. degree in electro-physics from the Polytechnic Institute of Brooklyn, Brooklyn, NY, USA, in 1968. In 1968, he held various research positions at the Polytechnic Institute of Brooklyn. From 1983 to 1990, he was a Professor of electrical engineering and the Director of the Electromagnetics Laboratory, New York Institute of Technology, Old Westbury. Since 1991, he has been a Professor of communication engineering at the National Chiao Tung University. Since September 1998, he has been the Director of the Microelectronics and Information Systems Research Center, National Chiao Tung University. He has been active in the field of general waveguiding structures and has published numerous papers on electromagnetics, optics, and acoustics. His current research interests include the guidance and scattering characteristics of periodic structures, antenna design, and electromagnetic compatibility. He is a member of Sigma Xi.

GUOBING ZHOU was born in Huzhou, Zhejiang, China, in 1994. He received the B.S. and M.S. degrees from the Zhejiang University of Technology, Zhejiang, in 2017 and 2021, respectively. Since 2021, he has been with Zhejiang Zhaolong Interconnect Technology Company Ltd., Deqing, China. His research interests include microwave, millimeter-wave, and subwavelength periodic structures.

LINFANG SHEN was born in Zhejiang, China, in 1965. He received the B.S. degree in physics from Peking University, Beijing, China, in 1986, the M.S. degree in plasma physics from the Institute of Plasma Physics, Academy of Science of China, Hefei, China, in 1989, and the Ph.D. degree in electronic engineering from the University of Science and Technology of China, in 2000. He is currently a Professor with the Zhejiang University of Technology. His research interests include surface plasmonics, photonic crystals, and metamaterials.

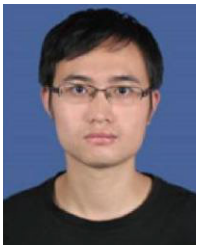

YUN YOU was born in Jiangxi, China, in 1990. He received the B.S., M.S., and Ph.D. degrees from Nanchang University, Nanchang, China, in 2012, 2015, and 2019, respectively. Since 2020, he has been working with the Department of Applied Physics, College of Science, Zhejiang University of Technology, Hangzhou, China. His research interests include surface magnetoplasmons, oneway waveguide, and 2D materials.

HANG ZHANG was born in Zhejiang, China. He received the Ph.D. degree in physics from Zhejiang University, Hangzhou, China, in 2002. He is currently an Associate Professor with the Department of Applied Physics, College of Science, Zhejiang University of Technology, Hangzhou. His research interests include free form optical design, semiconductor illumination, and the propagation of subwavelength periodic metal structures.